

# Distributed Associative Memory Network with Memory Refreshing Loss

Taewon Park<sup>a,\*</sup>, Inchul Choi<sup>b,\*</sup>, Minho Lee<sup>a,b,\*\*</sup>

<sup>a</sup>*Graduate School of Artificial Intelligence, Kyungpook National University, 80, Daehak-ro,  
Buk-go, Daegu, Republic of Korea*

<sup>b</sup>*NEOALI, 80, Daehak-ro, Buk-go, Daegu, Republic of Korea*

---

## Abstract

Despite recent progress in memory augmented neural network (MANN) research, associative memory networks with a single external memory still show limited performance on complex relational reasoning tasks. Especially the content-based addressable memory networks often fail to encode input data into rich enough representation for relational reasoning and this limits the relation modeling performance of MANN for long temporal sequence data. To address these problems, here we introduce a novel Distributed Associative Memory architecture (DAM) with Memory Refreshing Loss (MRL) which enhances the relation reasoning performance of MANN. Inspired by how the human brain works, our framework encodes data with distributed representation across multiple memory blocks and repeatedly refreshes the contents for enhanced memorization similar to the rehearsal process of the brain. For this procedure, we replace a single external memory with a set of multiple smaller associative memory blocks and update these sub-memory blocks simultaneously and independently for the distributed representation of input data. Moreover, we propose MRL which assists a task's target objective while learning relational information existing in data. MRL enables MANN to reinforce an association between input data and task objective by reproducing stochastically sampled input data from stored memory

---

\*Co-first authors with equal contribution

\*\*Corresponding author

*Email addresses:* [ptw7998@gmail.com](mailto:ptw7998@gmail.com) (Taewon Park), [sharpic77@gmail.com](mailto:sharpic77@gmail.com) (Inchul Choi), [mholee@gmail.com](mailto:mholee@gmail.com) (Minho Lee)

contents. With this procedure, MANN further enriches the stored representations with relational information. In experiments, we apply our approaches to Differential Neural Computer (DNC), which is one of the representative content-based addressing memory models and achieves the state-of-the-art performance on both memorization and relational reasoning tasks.

*Keywords:* Memory augmented neural network, relational reasoning, distributed representation, auxiliary loss, machine learning.

---

## 1. Introduction

The essential part of human intelligence for understanding the story and predicting unobserved facts largely depends on the ability to memorize the past and reasoning for relational information based on the pieces of memory. In this context, research on artificial intelligence has focused on designing a human-like associative memory network that can easily store and recall both events and relational information from a part of the information.

In neural network research, many approaches generally model sequential data with memory systems, such as Long Short Term Memory (LSTM) [1] or memory augmented neural networks (MANN). Especially, the recent approach in MANN constructs an associative memory with a content-based addressing mechanism and stores both input data and its relational information to a single external memory. MANN has already proven to be an essential component on many tasks which need long-term context understanding [2, 3, 4, 5, 6]. Also, compared to recurrent neural networks, it can store more information from sequential input data and correctly recall desired information from memory with a given cue. However, even with its promising performance on a wide range of tasks, MANN still has difficulties in solving complex relational reasoning problems [7]. Since the content-based addressing model implicitly encodes data items and their relational information into one vector representation, they often result in a lossy representation of relational information which is not rich enough for solving relational reasoning tasks. To address such weakness, some

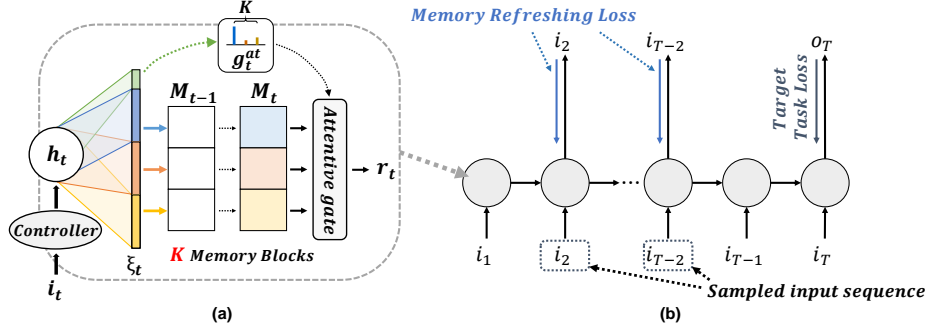


Figure 1: (a) The DAM with  $K$  sub-memory blocks (DAM-K) and attentive interpolation,  $g_t^{at}$ . (b) memory refreshing Loss.

researchers find relational information by leveraging interaction between memory entities with multi-head attention [8, 9]. Others focus on long sequence memorization performance of memory [10, 11, 12]. Another attempts to apply a self-attention to memory contents and explicitly encode relational information to a separate external memory [13]. However, all those models need to explicitly find relational information among memory entities with a highly computational attention mechanism and have to repeatedly recompute it on every memory update.

In this research, we approach the same problem in a much simpler and efficient way which is inspired by how our brain represents and restores information. We hypothesize that if we can encode input data into richer representations, MANN can provide enhanced relation modeling performance without exhaustive self-attention based relation searching. Based on this assumption, we find the weakness of the MANN model and facilitate it with the human brain-like mechanisms. One of the main weaknesses of conventional MANN is its lossy representation of relational information [13]. In terms of content-based addressing memory, it can be caused by both a single memory-based representation and long-temporal data association performance. Although MANN learns to correlate sequential events across time, its representation is not rich enough to reflect complex relational information existing in input data. Therefore, for the

enhanced relation learning, we focus on the richness of representation which implicitly embeds associations existing in input data. For this purpose, we introduce a novel Distributed Associative Memory (DAM) architecture which is inspired by how the information is represented in our brains [14, 15]. In DAM, we replace the single external memory with multiple smaller sub-memory blocks and update those memory blocks simultaneously and independently. The basic operations for each associative memory block are based on the content-based addressing mechanism of MANN, but its parallel memory architecture allows each sub-memory system to evolve over time independently. Through this procedure, the input information is encoded and stored in distributed representations. The distributed representation is a concept that stems from how the brain stores information in its neural networks and well known for its efficiency and powerful representational diversity. Furthermore, similar to the underlying insight of multi-head attention [16], our DAM model can jointly attend to information from different representation subspaces at different sub-memory blocks and is able to provide a more rich representation of the same common input data. To retrieve rich information for relational reasoning, we apply a soft-attention based interpolation to the diverse representations distributed across multiple memories.

Moreover, to enrich long-term relational information in the memory, we introduce a novel Memory Refreshing Loss (MRL) which fortifies relational modeling ability of the memory and generally enhances long-term memorization performance of MANN. The MRL forces the memory network to learn to reproduce the number of stochastically sampled input data only based on the stored memory contents. As if, other associated pieces of memory are reminded together whenever a person recalls a certain event in his memory, the data reproducing task enables MANN to have better association and memorization ability for input data. In our brain mechanisms, a similar concept is maintenance rehearsal operation which is repeatedly verbalizing or thinking about a piece of information. MRL is designed to reproduce a predefined percentage of input representations in the memory matrix on average and, while optimizing

two different tasks at the same time, keep the balance between MRL and target objective loss by dynamically re-weighting each task [17, 18].

By combining the above two approaches, DAM and MRL, our architecture provides rich representation which can be successfully used for tasks requiring both memorization and relational reasoning. We apply our architecture to Differential Neural Computer (DNC) [5], which is one of the representative content-based addressing memory, to construct novel distributed associative memory architecture with MRL. DNC has promising performance on diverse tasks but also known to be poor at complex relational reasoning tasks. In experiments, we show that our architecture greatly enhances both memorization and relation reasoning performance of DNC, and even achieves the state-of-the-art records.

## 2. Related Works

### 2.1. Biological Brain Mechanism

Our memory architecture is mainly inspired by the information processing mechanisms of the human brain. In our brain, forging new memories for facts and events, or retrieving information to serve the current task all depend on how information is represented and processed throughout the brain. In many researches [14, 15, 19, 20], there is already a broad consensus that distributed neural representations play a vital role in constructing and retrieving memories. For example, the first indications of the distributed character of memory in the cerebral cortex were provided in Lashley’s [14] neuropsychological experiments [21]. Also, this distributed representation concept is frequently applied for content-addressable memory, automatic generalization, adaptive rule selection [22]. Our model adopts this distributed representations concept with the multiple content-addressable memory network architecture to enrich the input data representation.

Moreover, in psychology researches, it is well known that human memory can be enhanced by repetitive rehearsal process of past information. Whether it is short-term or long-term memory, rehearsal can provide improved recall

performance and working memory for current task [23, 24]. Based on those researches, we design a new auxiliary loss function that is similar to the rehearsal process in our brain. Our loss function repetitively reconstructs some amount of previous input data based on the contents of memory while training for a target task. Since two different objectives are simultaneously trained with a multi-tasking learning setting, this procedure is comparable to the psychological case study when a person is intentionally rehearsing some information while recognizing its use for a different task. In our research, it is demonstrated that these biologically inspired contributions can effectively improve relational data modeling performance of memory augmented neural networks as in the human brain.

## 2.2. Neural Networks with Memory Augmentation

There are several MANN approaches that have focused on relation reasoning or long-term memorization enhancement of network. They can be categorized as follows.

*Multiple Memory based MANN.* In memory slot-based MANNs, the content-based addressing is implemented with a dynamic long-term memory which is composed of multiple memory slots [9, 25, 26, 27]. For multiple memory matrix-based models, researchers improve a single memory architecture by adding task-relevant information, asynchronous data input, and relational information to an additional memory matrix (e.g. dual memory) [13, 28, 29]. Our DAM adopts a multiple of the same type of memory matrix for distributed representation. Compared to other approaches, distributed memory architecture is much simpler and shows better performance on the same problems.

*Memory Networks for Relational Reasoning.* For relational reasoning, some MANN models explicitly find relational information by comparing their memory entities. Relational Memory Core (RMC) [9] leverages interaction mechanisms among memory entities to update memory with relational information. Self-attentive Associative Memory (STM) [13] adopts self-attention for memory

contents and store relational information to separate relation memory. Compared to those methods, DAM provides relational information through diverse representations of input data and long-term association performance of memory.

*Losses for Long-term Dependency.* For long-term memorization of the input pattern, [12] used a meta objective loss which forces a model to memorize input patterns in the meta-learning framework. Also, for longer sequence modeling, [10] adopted unsupervised auxiliary loss which reconstructs or predicts a sub-sequence of past input data. Compared to [10], MRL does not rely on a random anchor point and the sub-sequence reconstruction rather enforces memorization of every past input data that are associated with a target task. MRL focuses on enhancing data association while reproducing input representations, but also considering a balance with target objective loss by applying dynamic weighting method for dual-task optimization.

### 2.3. Differentiable Neural Computer

We first briefly summarize DNC architecture which is a baseline model for our approaches. DNC [5] is a memory augmented neural network inspired by conventional computer architecture and mainly consists of two parts, a controller and an external memory. When input data are provided to the controller, usually LSTM, it generates a collection of memory operators called as an interface vector  $\xi_t$  for accessing an external memory. It consists of several *keys* and *values* for read/write operations and constructed with the controller internal state  $\mathbf{h}_t$  as  $\xi_t = W_\xi \mathbf{h}_t$  at each time step  $t$ . Based on these memory operators, every read/write operation on DNC is performed.

During the writing process, DNC finds a writing address,  $\mathbf{w}_t^w \in [0, 1]^A$ , where  $A$  is a memory address size, along with writing memory operators, e.g. write-in *key*, and built-in functions. Then it updates write-in *values*,  $\mathbf{v}_t \in \mathbb{R}^L$ , in the external memory,  $\mathbf{M}_{t-1} \in \mathbb{R}^{A \times L}$ , along with erasing value,  $\mathbf{e}_t \in [0, 1]^L$ , where  $L$  is a memory length size as follows:

$$\mathbf{M}_t = \mathbf{M}_{t-1} \circ (\mathbf{E} - \mathbf{w}_t^w \mathbf{e}_t^\top) + \mathbf{w}_t^w \mathbf{v}_t^\top \quad (1)$$

where  $\circ$  denotes element-wise multiplication and  $\mathbf{E}$  is  $\mathbf{1}^{A \times L}$ .

In the reading process, DNC searches a reading address,  $\mathbf{w}_t^{r,i} \in [0, 1]^A$ , for  $R$  read heads, along with read memory operators, e.g. read-out *key*. Then, it reads out information from the external memory:

$$\mathbf{r}_t^i = \mathbf{M}_t \mathbf{w}_t^{r,i \top} \quad (2)$$

Finally, the output is computed as  $\mathbf{y}_t = W_y[\mathbf{h}_t; \mathbf{r}_t] \in \mathbb{R}^{d_o}$ , where  $\mathbf{r}_t = \{\mathbf{r}_t^i \in \mathbb{R}^L; 1 \leq i \leq R\}$ . Through these operations, DNC can learn how to store input data and utilize stored information to solve a given task. These whole mechanisms make DNC suitable for a general purposed memory augmented neural network.

### 3. Proposed Method

In this section, we introduce two methods that improve both memorization and relational reasoning ability of conventional DNC, a distributed associative memory architecture, and an MRL function. For a clear explanation, we illustrate DAM mechanism with a single read head case. For  $R$  read head cases of DAM, the details are in the Appendix.

#### 3.1. Distributed Associative Memory Architecture

The distributed associative memory architecture consists of a controller network and  $K$  associative memory blocks where each memory block is a content addressable memory similar to the original DNC [5]. Figure 1(a) shows the overall read/write process of the proposed DAM. For the writing operation, the controller of DAM produces multiple writing operator vectors for multiple memory blocks. Each writing operator vector is used for the content-based addressing of one of the multiple memory blocks, and it is independent of other memory blocks. Since it is produced based on the current input and previous hidden states of the controller, it can independently store its own representation of the same input contents. This writing process enables DAM to store



the diverse representations of the same input data to multiple memory blocks with much flexibility. Furthermore, for the reading process, all memory blocks are read at the same time and read values are interpolated with soft attention to produce single read-out information. Through this attention-based reading process, DAM retrieves the most suitable information for the current task from representations distributed in the multiple memory blocks. Based on these read/write operations, DAM learns how to store and retrieve the diverse representations of input data for different purposed tasks. The following sections detail the main operations.

### 3.1.1. Controller for Multiple Associative Memory Blocks

At each time step  $t$ , the controller receives an external input,  $\mathbf{i}_t$ , read-out of the previous time step,  $\mathbf{r}_{t-1}$ , and previous hidden state of controller,  $\mathbf{h}_{t-1}$ , to update its current hidden state,  $\mathbf{h}_t$ . After layer normalization, it produces an interface vector,  $\boldsymbol{\xi}_t \in \mathbb{R}^{K*(L*R+3L+3R+3)}$ , which includes read and write parameters for multiple memory access.

### 3.1.2. Write into Multiple Sub-Memory Blocks

The multiple memory writing processes in our architecture are based on the content-based memory accessing mechanism of DNC. A single memory block is addressed and updated with the same procedure of DNC, and such single memory block updating is applied to all blocks independently at the same time. As shown in Eq. (3), each memory block has its own interface vector relevant weight  $W_{\xi,1}, \dots, W_{\xi,k}$ , where  $k \in \{1, \dots, K\}$ . These weights are multiplied with a controller hidden state vector,  $\mathbf{h}_t$ , and used for memory operations of each independent memory block as following.

$$\boldsymbol{\xi}_t = [\boldsymbol{\xi}_{t,1}, \dots, \boldsymbol{\xi}_{t,K}, \hat{g}_t^{at}] = [W_{\xi,1}, \dots, W_{\xi,K}, W_{\xi,at}] \mathbf{h}_t \quad (3)$$

where  $\boldsymbol{\xi}_{t,k}$  is a interface vector for each memory block and  $\hat{g}_t^{at}$  is an attentive gate at time  $t$ .

Based on a writing operator obtained from  $\boldsymbol{\xi}_{t,k}$ , DAM updates input information into each memory block,  $\mathbf{M}_{t-1,k}$ , independently and simultaneously,

following Eq. (1). That independent and simultaneous writing procedures of sub-memory blocks allow that our DAM learns to construct diverse representations for the same common input data.

The following attention-based reading process is designed to integrate representations distributed across sub-memory blocks, and it contributes to enrich representation for relational reasoning tasks.

### 3.1.3. Read from Multiple Sub-Memory Blocks

As in the writing process, DAM obtains a reading operator from  $\xi_{t,k}$ , and computes reading address,  $\mathbf{w}_{t,k}^r \in [0, 1]^A$ , for each memory block. Based on those addresses, DAM reads values from each memory block and derives read-out value,  $\mathbf{r}_t \in \mathbb{R}^L$ , from them, using a processed attentive gate,  $g_t^{at} \in [0, 1]^K$ , as follows:

$$\mathbf{r}_t = \sum_{k=1}^K g_{t,k}^{at} \mathbf{M}_{t,k}^\top \mathbf{w}_{t,k}^r \quad (4)$$

where  $g_{t,k}^{at} = \text{Softmax}(\hat{g}_{t,k}^{at})$  for  $k = 1, \dots, K$ .

Compared to Eq. (2) of DNC, this reading process integrates representations stored in multiple memory blocks with the attentive gate and enables DAM to learn to provides the most appropriate distributed representation for a target task.

### 3.2. Memory Refreshing Loss

To enhance the relation modeling performance of a memory network, we design a novel auxiliary task, Memory Refreshing Loss (MRL), which can further improve the memorization performance of any given MANN. Our MRL function is inspired by the psychological case study on the rehearsal process of the human brain. In the study, if a person repeatedly rehearses given words or numbers while knowing its use for the following task, the overall memory performance is enhanced [23, 24, 30, 31]. Similarly, the main role of MRL task is forcing a memory network to reproduce sampled input data based on its memory content while training. When MRL task is trained with the main target task of the

model in a multi-task learning setting, main task-related representation, and its encoded association can be further emphasized while training [32, 33, 34, 35].

First, we define a task-specific target objective function,  $\mathcal{L}^{task}$ , of conventional MANN and MRL  $\mathcal{L}_t^{mr}$  as follows:

$$\mathcal{L}^{task} = \sum_{t=1}^T A(t) \ell_{task}(\mathbf{o}_t, \mathbf{y}_t) \quad (5)$$

where  $T$  is a whole sequence size,  $A(t)$  is a function at time  $t$ , which indicates whether current phase is in answer or not, if its value is 1, then  $t$  is in answer phases (otherwise 0).  $\mathbf{o}_t$  is a target answer and  $\ell_{task}(\cdot, \cdot)$  is a task target dependent loss function.

$$\mathcal{L}_t^{mr} = \ell_{mr}(\mathbf{i}_t, \mathbf{y}_t) \quad (6)$$

where  $\ell_{mr}(\cdot, \cdot)$  is an input sequence dependent loss function, and  $\mathbf{i}_t$  is an input,  $\mathbf{y}_t$  is an output at time step  $t$ , respectively.

Our MRL function is defined to use a sampled input sequence as its target data as shown in Eq. (6), and this procedure leads the model to refresh given input information while it is learning the given task. The error measure for MRL is adopted based on the input item type or main task characteristic. In this research, we use cross-entropy loss or  $L2$  loss depending on a given task.

As shown in Fig. 1(b), MRL forces a model to learn to reproduce sampled input sequences from stored representations in memory. When sampling input data, each item of input sequence is sampled with Bernoulli trial with probability,  $p$ , in which we call it as reproducing probability and it is defined as follows:

$$P(\alpha(t) = 1) = 1 - P(\alpha(t) = 0) = p \quad (7)$$

where  $\alpha(t)$  is an indicator function that represents sampling status at time  $t$ .

For an input sequence of length  $n$ , the series of Bernoulli trial-based samplings is the same as a Binomial sampling of the input sequence. Therefore, for any input sequence, on average,  $np$  samples are reconstructed by MRL because an expected value of Binomial sampling is a product between trial probability,

$p$ , and the number of trials,  $n$ . This random sampling policy prevents the model from learning to simply redirect given input to the output of the model at every time step.

When adding MRL to the task-specific target objective for multi-task learning, we also need a new strategy that can control the balance between MRL and original target task loss. Since, as the number of the story input increases, the MRL can overwhelm the total loss of the model. To prevent this loss imbalance problem, we apply a re-weighting method [18, 17], which dynamically keeps the balance between the target task objective  $\mathcal{L}^{task}$  and MRL  $\mathcal{L}^{mr}$ . Moreover, we also introduce a scaling factor,  $\gamma$ , to ensure the main portion of training loss can be the original target objective function.

$$\gamma = \begin{cases} \hat{\gamma} & \text{if } \hat{\gamma} \geq 1, \\ 1 & \text{otherwise.} \end{cases} \quad (8)$$

where  $\hat{\gamma} = \frac{\sum_{t=1}^T S(t)\alpha(t)}{\sum_{t=1}^T A(t)}$  and  $S(t)$  is an indicator function which represents whether current time step  $t$  is in the story phase or not. Finally, the total loss for the training of proposed model follows:

$$\mathcal{L} = \gamma \mathcal{L}^{task} + \sum_{t=1}^T \alpha(t) \mathcal{L}_t^{mr} \quad (9)$$

From above two memory related tasks,  $\mathcal{L}^{task}$  and  $\mathcal{L}^{mr}$ , while a model learns to reproduce input representations, target task-related representations and their association are further emphasized at the same time. As a result, MRL works as an auxiliary task that reinforces data association for a target objective.

#### 4. Experiments and Results

We evaluate each of our main contributions, Distributed Associative Memory architecture (DAM) and MRL, separately for ablation study, and show the performance of DAM-MR for complex relational reasoning tasks, such as bAbI,  $N^{th}$  farthest task, and Convex hull task. In all experiments, we adopt well-known neural network generalization techniques that are used in [36] for our

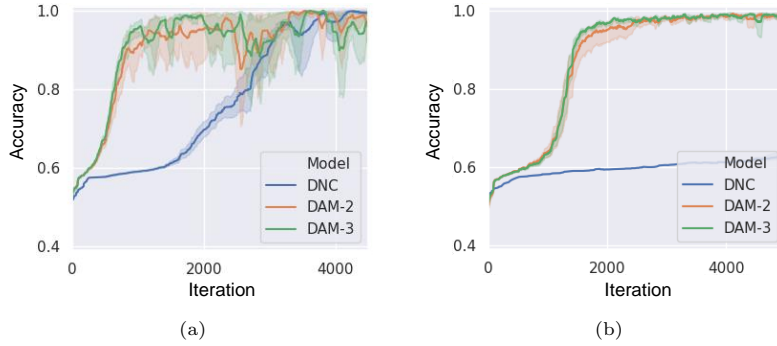


Figure 2: Mean training curves on the algorithmic tasks which are (a) the copy task and (b) the associative recall task. The shadowed area shows a standard deviation of 10 trials.

baseline DNC model. The detailed parameter settings and adopted generalization techniques are shown in the Appendix.

#### 4.1. Distributed Associative Memory Architecture Evaluation

The distributed memory architecture is evaluated in three aspects. First, we show the verification of the basic memory network capability of DAM with Algorithmic tasks. Second, for the evaluation of memory efficiency in data association performance, DAM is configured to have a similar total memory size as a single memory model and evaluated with the Representation Recall task. Third, scalability experiments of DAM show the effect of the number of sub-memory blocks on the relation reasoning performance. In this experiment, we represent DAM architecture with  $K$  sub memory blocks as DAM- $K$ . The scalability experiments are performed with two settings, one is iteratively dividing a fixed total memory size to obtain multiple sub-memory blocks, the other is use a fixed sub-memory block size and adopting additional sub-memory blocks while increasing total memory size.

##### 4.1.1. Algorithmic Tasks

We show the effect of DAM on the basic memory network performance with the copy and the associative recall tasks from [4]. The copy task is designed to show whether a model can store and recall arbitrary long sequential data

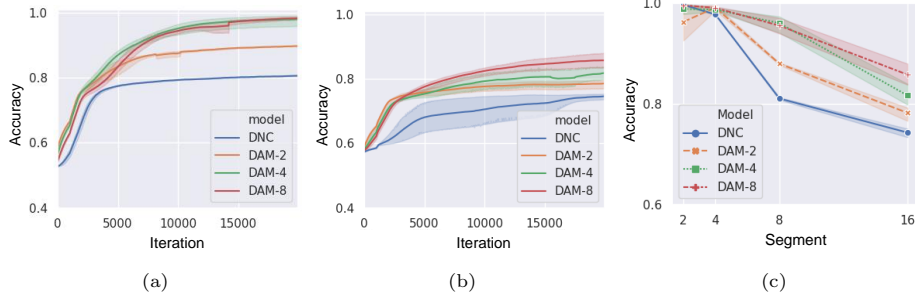


Figure 3: Mean training curves for (a) 8 segment and (b) 16 segment on the Representation Recall task. (c) Mean accuracy of DAM models on the Representation Recall task. The shadowed area shows a standard deviation of 10 trials.

correctly, and the associative recall task is intended to show whether a model can recall the information associated with a given cue by remembering temporal relation between input data. As shown in Fig. 2, simply adopting DAM architecture enhances the relation recall performance of the memory model. We can obtain more benefits by adding additional sub-memory blocks to DAM architecture (by increasing  $K$ , from 2 to 3), however, for the copy task, as shown in Fig. 2(a), the effect of the number of memory blocks is small because it is not a task designed for the evaluation of relation reasoning, rather focusing on simple memorization performance.

#### 4.1.2. Representation Recall Task

We design a new algorithmic task, called a Representation Recall (RR) task, which evaluates how much representation details a memory model can remember and recall from memory. This task uses randomly generated binary vectors as input sequences. From the sequence, a binary vector is randomly selected and divided into  $2N$  sub-parts. Among them,  $N$  sub-parts are provided as a cue for a model to predict the rest of the sub-parts. In order to solve this task, the model is required to remember  $\frac{2N!}{N!(2N-N)!}$  combinations of relations existing in each input, and therefore task complexity increases as  $N$  increases. To show the efficiency of a model with a fair comparison, we configure DAM by dividing the original single external memory into the group of 1/2, 1/4, and 1/8 sized

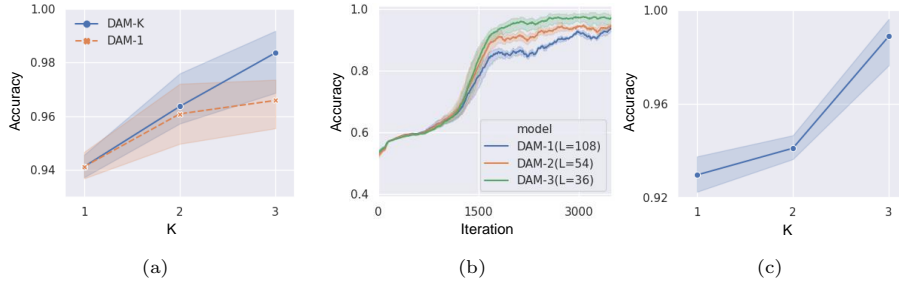


Figure 4: Scalability Experiments with Associative Recall task. (a) Scalability test while increasing single memory size. (b) Training curve while iteratively dividing a fixed memory size. (c) Scalability test while iteratively dividing a fixed memory size.

sub-memory blocks. The mean training curves of DAM- $K$  ( $K=2, 4$ , and  $8$ ) are compared with the original DNC while increasing the task complexity  $N$  as in shown Figs. 3(a) and (b). The result demonstrates that our proposed architecture learns the task much faster than other DNC based models, and also shows better accuracy and learning stability (smaller standard deviation in learning curve). Furthermore, we compared the final accuracy of DAM- $K$  ( $K=2, 4$ , and  $8$ ) on RR task while increasing the task complexity from 2 to 16 segments. As shown in Fig. 3(c), if task complexity increases, the final accuracy inevitably degrades. However, DAM with more sub-memory blocks suffers less performance degradation. Although all of the models have the same total memory size, a DAM model with more sub-memory blocks provides richer representation which includes more details of input.

#### 4.1.3. Scalability Experiments

*Associative Recall task.* We perform a scalability experiment on the associative recall task with fixed memory address size  $A = 16$ . We set the memory length  $L$  of a sub-memory block to 108, 54, and 36, and compares the performance of DAM according to the number of sub-memory blocks,  $K$  in Figure 4. The result shown in Figure 4(a) corresponds to the case when a single memory size of DAM-1 is linearly increased and the same total memory size is divided to obtain multiple smaller memory blocks for DAM-2 and 3. As shown in the results, the

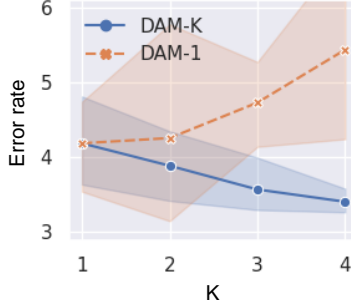


Figure 5: Mean error rate of DAM models on the bAbI task.

model with a smaller memory block size provides more accuracy. Figure 4(c) shows the case when we adopt a single fixed total memory size for DAM-1, 2, and 3, and each of DAM-2 and 3 represents the number of sub-memory blocks under the same condition. Similar to Fig. 4(a), as we divide the memory size to obtain more sub-memory blocks, better accuracy is obtained if there is no information loss at a single sub-memory block. Figure 4(b) shows the training curves for the case of Fig. 4(c). It shows DAM architecture can expedite the training speed of the model even with the smaller number of memory slots.

*bAbI task.* For the evaluation of the scalability of distributed associative memory architecture without the effect of information loss at a sub-memory block, we adopt a fixed size sub-memory block that has a larger length than a half of the input size and then increase the number of sub-memory blocks to produce several models, DAM-2, 3, and 4. We evaluate all model’s performance with complex reasoning tasks, bAbI task, to show the effect of  $K$  (representation diversity) on relational reasoning performance. The bAbI task [7] is a set of 20 different tasks for evaluating text understanding and reasoning, such as basic induction and deduction. In Fig. 5, the DAM-1 represents a baseline model that has a single external memory and includes modifications from [36] for the generalization performance enhancement. For the comparison with DAM- $K$  ( $K=2, 3$ , and 4), we linearly increase its single external memory size. The overall graph



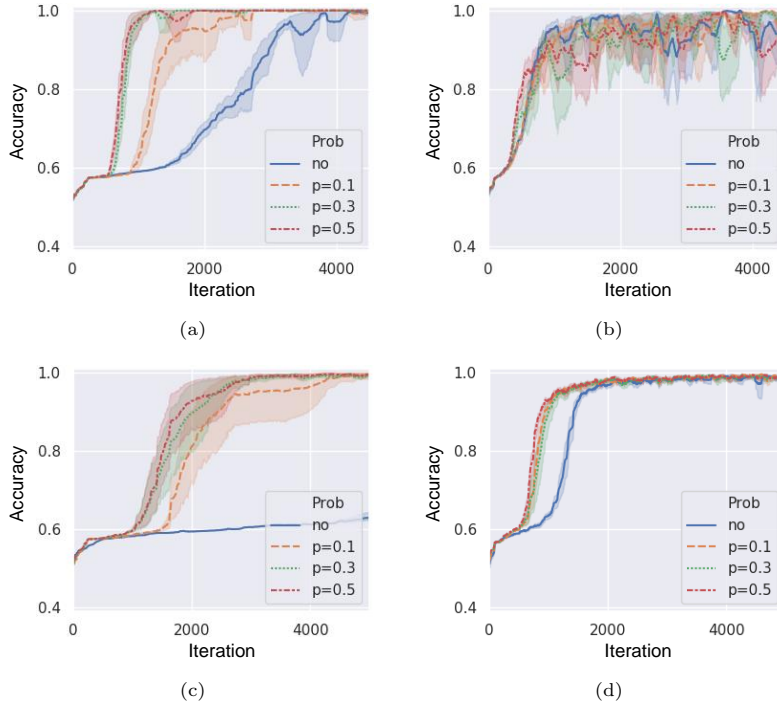


Figure 6: Mean training curves for different reproducing probability values at (a) DNC and (b) DAM-3 on the copy task. Mean training curves for different reproducing probability values at (c) DNC and (d) DAM-3 on the associative recall task. The shadowed area shows a standard deviation of 10 trials.

shows that, as the degree of distribution increases, performance on bAbI tasks is also enhanced accordingly for both mean error rate and standard deviation of results. If we use more sub-memory blocks to further increase  $K$ , we can obtain gradual performance enhancement, which clearly shows the benefits of distributed associative memory architecture.

#### 4.2. Memory Refreshing Loss Evaluation

To show the effect of MRL on MANN, we apply it to Algorithmic Tasks (Copy and Associative Recall task). In Fig. 6, we show the mean training curves according to the reproducing probability,  $p$ , on the copy task, and the associative recall task, respectively. For DAM-MR, although we show only DAM3-MR,

other configurations (DAM2-MR, DAM4-MR) have similar results. As shown in Fig. 6, the MRL function expedites the learning speed of models in most cases. For the original DNC, it makes the training speed of model much faster and it is further increased by the high reproducing probability on both tasks. For DAM-MR, the MRL enhances the training speed of the models but DAM is not sensitive to the change of reproducing probability. From those results, we can see that the effect of MRL is related to the property of a given task.

#### 4.3. DAM-MR Evaluation on Relational Reasoning Tasks

As shown in the ablation study, each component of the proposed architecture has a significant impact on the original DNC performance. To show the performance of the whole combined model, DAM-MR, we compare our architecture to other DNC’s variations and attention-based MANN on following relational reasoning tasks. To support our argument on the relational information retrieving approach, we adopt recent memory network models which are applying extensive self-attention [13] or multi-head attention for encoding relational information [9] as our counterparts. Specifically, Self-attentive Associative Memory (STM) [13], Relational Memory Core (RMC) [9] and Universal Transformer (UT) [37] use self-attention and multi-head attention in their memory architecture.

##### 4.3.1. $N^{th}$ Farthest

This task evaluates a model capacity for relational reasoning across time. It asks a model to find the  $N^{th}$  farthest vector from a given query vector, and this requires the memorization of relational information between vectors, such as distance, and sorting mechanism. With this task, the long temporal relation modeling performance of a model can be demonstrated.

Table 1 shows a comparison of the  $N^{th}$  Farthest task results between our model and other MANN models which are designed for relational reasoning tasks. In the results, even though the original DNC can not solve the task at all, our DAM-MR shows surprisingly high performance on the task. Even compared to Relational Memory Core (RMC) [9], which explicitly finds relational

Table 1: Test accuracy [%] on  $N^{th}$  Farthest task.

Model	Accuracy
DNC [9]	25
RMC [9]	91
TPR [13]	13
STM [13]	98
RMC-MR ( $p = 0.3$ )	94
DARMC4-MR ( $p = 0.3$ )	<b>98.2</b>
DAM6-MR ( $p = 0.3$ )	97.8

information from memory based on multi-head attention mechanism, DAM6-MR shows superior performance. For STM [13], our model shows a slightly lower accuracy. However, if we consider STM’s self-attention computations for finding every possible relation with outer products, our DAM-MR is a quite simple and efficient architecture that does not introduce any explicit relation seeking operations or high-order storage. Therefore, in the aspect of model efficiency, DAM-MR is showing a novel way of modeling relational information which is a promising alternative for self-attention based approach. Moreover, if we apply our DAM architecture and MRL to the RMC, it even shows better performance than STM. Although RMC already has its own way of searching relational information from its memory, which overlaps with DAM’s purpose, our DAM-MR provides further performance improvement on the task. This result demonstrates the additional benefit of DAM architecture as a generally applicable design choice for MANN.

Table 2: Test accuracy [%] on Convex hull task.

Model	$N = 5$	$N = 10$
LSTM [13]	89.15	82.24
ALSTM [13]	89.92	85.22
DNC [13]	89.42	79.47
RMC [13]	93.72	81.23
STM [13]	96.85	91.88
<b>DAM6-MR</b> ( $p = 0.3$ )	95.6	89.8
<b>DAM8-MR</b> ( $p = 0.3$ )	95.4	90.5
<b>DARMC8-MR</b> ( $p = 0.3$ )	<b>97.2</b>	<b>92.3</b>

#### 4.3.2. Convex hull task

The convex hull task [41] is predicting a list of points that forms a convex hull sorted by coordinates. The input list consists of  $N$  points with 2D coordinates. In this experiment, we train the model with  $N \in [5, 20]$  and test with  $N = 5, 10$  cases. The output is a sequence of 20-dimensional one-hot vectors representing the features of the solution points in the convex-hull. As shown in Table 2, DAM-MR shows better accuracy than RMC [9] and similar performance with STM [13]. Moreover, DARMC-MR, which is DAM applied RMC, shows even better performance than STM, which also demonstrates the effectiveness and generality of our DAM architecture.

#### 4.3.3. bAbI QA task

The bAbI task [7] is a set of 20 different tasks for evaluating text understanding and reasoning, such as basic induction and deduction. Each task consists of stories for questions and correct answers for the questions, e.g. *Daniel travelled to the bathroom. Mary moved to the office. Where is Daniel? bathroom.* In evaluation, a model is supposed to remember the story and recall related information to provide correct answer for the given questions.

Table 3: The mean word error rate [%] for 10 runs of different DNC based models trained jointly on all 20 bAbI task.

Model	Mean	Best
DNC [5]	$16.7 \pm 7.6$	3.8
SDNC [38]	$6.4 \pm 2.5$	2.9
rsDNC [36]	$6.3 \pm 2.7$	3.6
DNC-MD [39]	$9.5 \pm 1.6$	n/a
NUTM [40]	$5.6 \pm 1.9$	3.3
<b>DAM2-MR</b> ( $p = 0.1$ )	$1.5 \pm 1.3$	0.16
<b>DAM2-MR</b> ( $p = 0.3$ )	$2.5 \pm 1.0$	<b>0.14</b>

Table 3 shows experimental results on the bAbI task. In this experimental result, our proposed model, DAM2-MR with  $p = 0.1$ , shows the best mean performance on the bAbI task, among all other DNC based approaches. These results demonstrate that our proposed architecture efficiently learns the bAbI task by using distributed associative memory architecture and memory refreshing loss. Particularly, in Table 4, the best result of DAM2-MR records the state-of-the-art performance on the bAbI task, even compared to other types of recent MANN models.

## 5. Conclusion

In this paper, we present a novel DAM architecture and an MRL function to enhance the data association performance of memory augmented neural networks. The proposed distributed associative memory architecture stores input contents to the multiple sub-memory blocks with diverse representations and retrieves required information with soft-attention based interpolation over multiple distributed memories. We introduce a novel MRL to explicitly improve the long-term data association performance of MANN. Our MRL is designed

Table 4: The mean word error rate [%] for best run of MAMN models trained jointly on all 20 bAbI tasks.

Model	Best
Transformer [37]	22.1
UT [37]	0.29
MNM-p [12]	0.175
MEMO [42]	0.21
STM [13]	0.15
<b>DAM2-MR</b> ( $p = 0.1$ )	0.16
<b>DAM2-MR</b> ( $p = 0.3$ )	<b>0.14</b>

to reproduce the contents of associative memory with sampled input data and also provides a dynamic task balancing with respect to the target objective loss. We implement our novel architecture with DNC and test its performance with challenging relational reasoning tasks. The evaluation results demonstrate that our DAM-MR correctly stores input information and robustly recalls the stored information based on the purpose of the given tasks. Also, it shows that our model not only improves the learning speed of DNC, but reinforces the relation reasoning performance of the model. Eventually, our DAM-MR significantly outperforms all other variations of DNC and shows the state-of-the-art performance on complex relation reasoning tasks, bAbI, even compared to other types of memory augmented network models. As future works, we are going to optimize the task balancing strategy between MRL and target loss, and perform further research on how MRL affects multiple sub-memory blocks while optimizing the memory model.

## Acknowledgment

This work was partly supported by the National Research Foundation of Korea(NRF) grant funded by the Korea government(MSIT) (No. 2021R1A2C3011169) (50%). It was also supported by Electronics and Telecommunications Research Institute(ETRI) grant funded by the Korean government. [21ZS1100, Core Technology Research for Self-Improving Integrated Artificial Intelligence System](50%).

## References

- [1] S. Hochreiter, J. Schmidhuber, Long short-term memory, *Neural computation* 9 (8) (1997) 1735–1780.
- [2] J. Weston, S. Chopra, A. Bordes, Memory networks, *arXiv preprint arXiv:1410.3916*.
- [3] S. Sukhbaatar, J. Weston, R. Fergus, et al., End-to-end memory networks, in: *Advances in neural information processing systems*, 2015, pp. 2440–2448.
- [4] A. Graves, G. Wayne, I. Danihelka, Neural turing machines, *arXiv preprint arXiv:1410.5401*.
- [5] A. Graves, G. Wayne, M. Reynolds, T. Harley, I. Danihelka, A. Grabska-Barwińska, S. G. Colmenarejo, E. Grefenstette, T. Ramalho, J. Agapiou, et al., Hybrid computing using a neural network with dynamic external memory, *Nature* 538 (7626) (2016) 471.
- [6] C. Gulcehre, S. Chandar, K. Cho, Y. Bengio, Dynamic neural turing machine with continuous and discrete addressing schemes, *Neural computation* 30 (4) (2018) 857–884.
- [7] J. Weston, A. Bordes, S. Chopra, A. M. Rush, B. van Merriënboer, A. Joulin, T. Mikolov, Towards ai-complete question answering: A set of prerequisite toy tasks, *arXiv preprint arXiv:1502.05698*.

- [8] R. Palm, U. Paquet, O. Winther, Recurrent relational networks, in: Advances in Neural Information Processing Systems, 2018, pp. 3368–3378.
- [9] A. Santoro, R. Faulkner, D. Raposo, J. Rae, M. Chrzanowski, T. Weber, D. Wierstra, O. Vinyals, R. Pascanu, T. Lillicrap, Relational recurrent neural networks, in: Advances in neural information processing systems, 2018, pp. 7299–7310.
- [10] T. H. Trinh, A. M. Dai, M.-T. Luong, Q. V. Le, Learning longer-term dependencies in rnns with auxiliary losses, arXiv preprint arXiv:1803.00144.
- [11] H. Le, T. Tran, S. Venkatesh, Learning to remember more with less memorization, arXiv preprint arXiv:1901.01347.
- [12] T. Munkhdalai, A. Sordoni, T. Wang, A. Trischler, Metalearned neural memory, in: Advances in Neural Information Processing Systems, 2019, pp. 13310–13321.
- [13] H. Le, T. Tran, S. Venkatesh, Self-attentive associative memory, arXiv preprint arXiv:2002.03519.
- [14] K. S. Lashley, In search of the engram.
- [15] D. Bruce, Fifty years since lashley’s in search of the engram: Refutations and conjectures, Journal of the History of the Neurosciences 10 (3) (2001) 308–318, pMID: 11770197. arXiv:<https://www.tandfonline.com/doi/pdf/10.1076/jhin.10.3.308.9086>, doi:10.1076/jhin.10.3.308.9086.  
URL <https://www.tandfonline.com/doi/abs/10.1076/jhin.10.3.308.9086>
- [16] A. Vaswani, N. Shazeer, N. Parmar, J. Uszkoreit, L. Jones, A. N. Gomez, L. Kaiser, I. Polosukhin, Attention is all you need, in: Advances in neural information processing systems, 2017, pp. 5998–6008.



- [17] X.-Y. Liu, Z.-H. Zhou, The influence of class imbalance on cost-sensitive learning: An empirical study, in: Sixth International Conference on Data Mining (ICDM'06), IEEE, 2006, pp. 970–974.
- [18] Y. Cui, M. Jia, T.-Y. Lin, Y. Song, S. Belongie, Class-balanced loss based on effective number of samples, in: Proceedings of the IEEE Conference on Computer Vision and Pattern Recognition, 2019, pp. 9268–9277.
- [19] F. Crick, G. Mitchison, The function of dream sleep, *Nature* 304 (5922) (1983) 111–114.
- [20] R. F. Thompson, Are memory traces localized or distributed?, *Neuropsychologia* 29 (6) (1991) 571–582.
- [21] J. M. Fuster, Distributed memory for both short and long term, *Neurobiology of Learning and Memory* 70 (1-2) (1998) 268–274.
- [22] G. E. Hinton, Distributed representations.
- [23] D. Rundus, Maintenance rehearsal and long-term recency, *Memory & Cognition* 8 (3) (1980) 226–230.
- [24] R. L. Greene, Effects of maintenance rehearsal on human memory., *Psychological Bulletin* 102 (3) (1987) 403.
- [25] I. Danihelka, G. Wayne, B. Uria, N. Kalchbrenner, A. Graves, Associative long short-term memory, arXiv preprint arXiv:1602.03032.
- [26] M. Henaff, J. Weston, A. Szlam, A. Bordes, Y. LeCun, Tracking the world state with recurrent entity networks, arXiv preprint arXiv:1612.03969.
- [27] A. Goyal, A. Lamb, J. Hoffmann, S. Sodhani, S. Levine, Y. Bengio, B. Schölkopf, Recurrent independent mechanisms, arXiv preprint arXiv:1909.10893.
- [28] T. Munkhdalai, H. Yu, Neural semantic encoders, in: Proceedings of the conference. Association for Computational Linguistics. Meeting, Vol. 1, NIH Public Access, 2017, p. 397.

- [29] H. Le, T. Tran, S. Venkatesh, Dual memory neural computer for asynchronous two-view sequential learning, in: Proceedings of the 24th ACM SIGKDD International Conference on Knowledge Discovery & Data Mining, 2018, pp. 1637–1645.
- [30] A. S. Souza, L. Rerko, K. Oberauer, Refreshing memory traces: Thinking of an item improves retrieval from visual working memory, *Annals of the New York Academy of Sciences* 1339 (1) (2015) 20–31.
- [31] V. Camos, P. Lagner, V. M. Loaiza, Maintenance of item and order information in verbal working memory, *Memory* 25 (8) (2017) 953–968.
- [32] R. Caruana, V. R. De Sa, Promoting poor features to supervisors: Some inputs work better as outputs, in: Advances in Neural Information Processing Systems, 1997, pp. 389–395.
- [33] S. Ben-David, R. Schuller, Exploiting task relatedness for multiple task learning, in: Learning Theory and Kernel Machines, Springer, 2003, pp. 567–580.
- [34] H. M. Alonso, B. Plank, When is multitask learning effective? semantic sequence prediction under varying data conditions, *arXiv preprint arXiv:1612.02251*.
- [35] M. Rei, Semi-supervised multitask learning for sequence labeling, *arXiv preprint arXiv:1704.07156*.
- [36] J. Franke, J. Niehues, A. Waibel, Robust and scalable differentiable neural computer for question answering, *arXiv preprint arXiv:1807.02658*.
- [37] M. Dehghani, S. Gouws, O. Vinyals, J. Uszkoreit, L. Kaiser, Universal transformers, *arXiv preprint arXiv:1807.03819*.
- [38] J. Rae, J. J. Hunt, I. Danihelka, T. Harley, A. W. Senior, G. Wayne, A. Graves, T. Lillicrap, Scaling memory-augmented neural networks with

- sparse reads and writes, in: *Advances in Neural Information Processing Systems*, 2016, pp. 3621–3629.
- [39] R. Csordás, J. Schmidhuber, Improving differentiable neural computers through memory masking, de-allocation, and link distribution sharpness control, arXiv preprint arXiv:1904.10278.
  - [40] H. Le, T. Tran, S. Venkatesh, Neural stored-program memory, in: *International Conference on Learning Representations*, 2020.  
URL <https://openreview.net/forum?id=rkxxA24FDr>
  - [41] O. Vinyals, M. Fortunato, N. Jaitly, Pointer networks, in: *Advances in neural information processing systems*, 2015, pp. 2692–2700.
  - [42] A. Banino, A. P. Badia, R. Köster, M. J. Chadwick, V. Zambaldi, D. Hassabis, C. Barry, M. Botvinick, D. Kumaran, C. Blundell, Memo: A deep network for flexible combination of episodic memories, in: *International Conference on Learning Representations*, 2020.  
URL <https://openreview.net/forum?id=rJxlc0EtDr>
  - [43] J. Lei Ba, J. R. Kiros, G. E. Hinton, Layer normalization, arXiv preprint arXiv:1607.06450.
  - [44] N. Srivastava, G. Hinton, A. Krizhevsky, I. Sutskever, R. Salakhutdinov, Dropout: a simple way to prevent neural networks from overfitting, *The journal of machine learning research* 15 (1) (2014) 1929–1958.

## Appendix A. Experiment Details

In experiments, for model optimization, we adopt an RMSprop optimizer with a momentum value as 0.9 and epsilon as  $10^{-10}$ .

### Appendix A.1. Model Configuration Details

#### Appendix A.1.1. Distributed Associative Memory Architecture for DNC

We configure hyper-parameters of our model with two types of settings, one for the comparison with other memory network models and the other for the scalability experiment of distributed memory (DM). For the comparison with other models, we keep the almost same total memory size of DNC and divide it into smaller sub-memory blocks to construct a distributed memory system for a fair comparison. Also, we adjust the memory length size of DAM so that it has a similar amount of trainable parameters with other DNC variants. Tables A.1 and A.2 show our model hyper-parameters for each task, including a controller’s internal state,  $d_h$ , the number of read heads,  $R$ , the number of memory blocks,  $K$ , a memory address size,  $A$  and a memory length size,  $L$ .

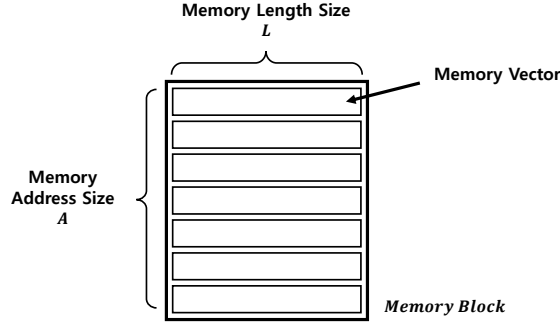


Figure A.1: Composition of a memory block.

For the scalability evaluation of DAM, we set the memory length of a single sub-memory block,  $L$ , same as the memory block size of DAM-2. The size smaller than this causes the information loss because of too small memory matrix size compared to the input length. In this configuration, we increase the

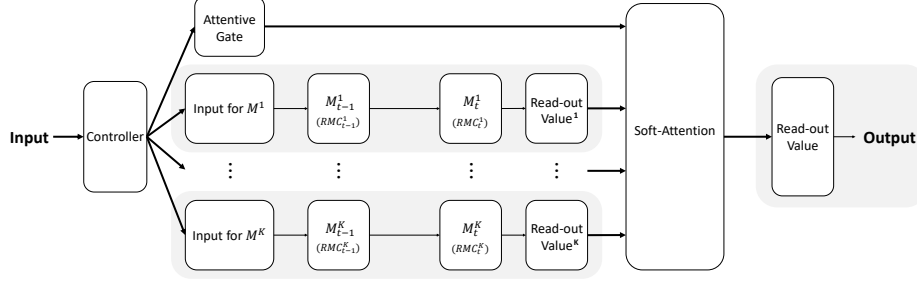


Figure A.2: The Distributed Associative Memory architecture applied RMC (DAMRMC). Each sub memory block can be replaced by any MANN model.

degree of distribution by increasing the number of sub-memory blocks. Since we fix the single memory block size, the total memory size increases linearly with  $K$ . Table A.3 shows the details of configuration.

#### Appendix A.1.2. Distributed Associative Memory Architecture for RMC

To show the effectiveness and generality of our DAM architecture, we naively apply DAM architecture to RMC [9] by constructing a memory system with the collection of several RMC blocks, as shown in Fig. A.2. By treating a single RMC memory network as a single sub memory block, we compose a memory architecture with  $K$  memory blocks. For DAM operations, we add a controller network (feed-forward network) to provide input value to the multiple memory blocks, and for the memory read-out, integrate the read-out value of each memory block with attentive-gate based soft-attention mechanism. We set the hyper-parameters of each RMC memory block as 8 memory slots with 1,536 total units and 6 heads for the  $N^{th}$  Farthest task, and 8 memory slots with 2,048 total units and 8 heads for the convexhull task.

#### Appendix A.2. Experimental Task Explanation

In this subsection, we introduce our experimental setup and how to conduct experiments on each task.

### Appendix A.2.1. Algorithmic Task Description

The experiments on algorithmic tasks are repeated 10 times with a batch size of 16 and a learning rate of  $10^{-4}$ , and training iterations of 20K on Representation Recall task and training iterations of 10K on Copy and Associative Recall tasks. We evaluate the performance on the algorithmic tasks based on the accuracy which is defined as  $L1$  norm between model outputs and targets. In each task, an input flag is provided with story (input) data which are required to produce an answer. After story input, query data along with the output flag are provided to the model. Based on the input and stored information, the model is required to predict an correct answer. For training, we randomly construct each task’s data at each iteration as the following configurations.

*Representation Recall Task..* In this task,  $L_i$  binary vectors, each has  $W$  length, are randomly generated and are provided to the model along with an input flag. Here, we divide each input binary vector into  $2N$  segments and use the half of them,  $N$ , as a cue vector. For an answer phase,  $L_c$  cue vectors are constructed by random sampling from  $L_i$  binary vectors with replacement and  $N$  segments without replacement. The network has to predict the remaining  $N$  segments when each cue vector is provided. We use  $L_i = 8$ ,  $W = 64$ ,  $N \in \{2, 4, 8\}$ , and  $L_c \in [8, 16]$ . Therefore,  $d_i$  and  $d_o$  are 64 and 32, respectively.

*Copy Task and Associative Recall Task..* In the copy task [4],  $L_i$  binary vectors, each has  $W$  length, are randomly generated and are provided to the model along with an input flag. After receiving an output flag, the model is required to sequentially produce the same  $L_i$  binary vectors as an output. We use  $W = 8$  and the number of binary vectors,  $L_i \in [8, 32]$ , is randomly chosen at each iteration. In the associative task [4], we define an item as a sequence of binary vectors with width  $W$ , and during the input phase,  $L_i$  input items, each consists of  $N_i$  binary vectors, are provided to a model along with an input flag. Subsequently, a query item, which is randomly chosen from an input item sequence, is provided to the model along with an output flag. In this phase, the model is required to predict a subsequent item that has placed right after the query item

Table A.1: Model hyper-parameters for the copy task, associative recall task, and bAbI task.

Hyper parameter	Copy		Associative Recall		bAbI QA
	DNC	DAM-K	DNC	DAM-K	DAM-2
$d_h$	128	128	128	128	256
$R$	1	1	1	1	4
$K$	1	{2, 3}	1	{2, 3}	2
$A$	64	64	32	32	128
$L$	36	36	36	36	48
Memory Capacity	2.3K	{4.6K, 6.9K}	1.1K	{2.3K, 3.4K}	12.3K
Total Parameters	0.11M	{0.13M, 0.15M}	0.11M	{0.13M, 0.15M}	0.79M

in the input item sequence. We use  $W = 8$ ,  $N_i = 3$ , and the number of items,  $L_i \in [2, 8]$ , is randomly chosen at each iteration. Therefore,  $d_i$  and  $d_o$  are 10 on both tasks.

#### Appendix A.2.2. bAbI Task

Our experiments on bAbI task are repeated 10 times with a batch size of 32 and a learning rate of  $[1, 3, 10] \times 10^{-5}$ , and we fine-tuned a model with the learning rate of  $10^{-5}$  and training iterations of 10K. We compose experimental set on the bAbI task with 62,493 training samples and 6,267 testing samples and adopt fixed training iterations of about 0.1M. We use a word embedding, which is a general method in a natural language processing domain, with an embedding size of 64. Thus,  $d_i$  is 64 and  $d_o$  is 160. We evaluate the performance on the bAbI task based on the word error rate for answer words in the test samples.

*Pre-processing on bAbI Task Dataset.* The bAbI task dataset [7] consists of many different types of sets that share similar properties. Among them, we only use en-10K set to fairly compare the performance with other researches. In data pre-processing, any input sequences which have more than 800 words are all excluded from the training dataset as in [36] for computational efficiency. After the exclusion, we construct our dataset with 62,493 training

Table A.2: Model hyper-parameters for the representation recall task,  $N^{th}$  farthest task, and the convex hull task.

Hyper parameter	Representation Recall		$N^{th}$ Farthest	Convex Hull
	DNC	DAM-K	DAM-6	DAM-K
$d_h$	128	128	1024	256
$R$	1	1	4	4
$K$	1	{2, 4, 8}	6	{6, 8}
$A$	32	32	16	20
$L$	256	256/ $K$	128	64
Memory Capacity	8.2K	8.2K	12.3K	{7.7K, 10.2K}
Total Parameters	0.38M	{0.31M, 0.27M, 0.26M}	12.6M	{1.5M, 1.7M}

samples and 6,267 testing samples. We remove all numbers from input data and split every sentence into words, and convert every word to its corresponding lower case. After these processes, the whole vocabulary composed of 156 unique words and four symbols, which are '[PAD]', '?', '.', and '-'. The '-' symbol represents that the model has to predict an answer word at the current time step. Therefore, answer words are replaced to '-' symbol from input data. The bAbI task dataset is available on [http://www.thespermwhale.com/jaseweston/babi/tasks\\_1-20\\_v1-2.tar.gz](http://www.thespermwhale.com/jaseweston/babi/tasks_1-20_v1-2.tar.gz).

#### Appendix A.2.3. $N^{th}$ Farthest task

We use the same task configuration used in [9], which uses Adam Optimizer with a batch size of 1,600 and an initial learning rate of  $1e^{-4}$ , consists of eight 16-dimensional input vectors, and add 4-layers of MLP with ReLU activation function to the output layer. We set DAM configurations as shown in Table A.2.

#### Appendix A.2.4. Convex hull task

We use the same task configuration used in [13], which adopts RMSProp Optimizer with a batch size of 128 and an initial learning rate of  $1e^{-4}$ . We add



Table A.3: Model hyper-parameters for scalability evaluation on the bAbI task.

Hyper parameter	DAM-1	DAM-2	DAM-3	DAM-4
$d_h$	256	256	256	256
$R$	4	4	4	4
$K$	1	2	3	4
$A$	192	128	128	128
$L$	64	48	48	48
Memory Capacity	12.3K	12.3K	18.4K	24.6K
Total Parameters	0.80M	0.79M	0.88M	0.97M

2-layers of MLP with ReLU activation function (each layer has 256 units) to the output layer and set DAM configurations as shown in Table A.2.

## Appendix B. Additional Analysis of Memory Refreshing Loss

Proposed Memory Refreshing Loss (MRL) chooses a subset of input sequence based on a stochastic sampling with trial probability,  $p$ , which is called a reproducing probability. It adaptively decides the number of sampled input story,  $n'$ , according to the story sequence length,  $n$ , by adjusting this reproducing probability. Since it is a binomial sampling with independent trials, the expected sampled story length is as shown in Eq. (B.1). Therefore, it can consistently enhance the memorization performance of memory with the reproducing probability of  $p$ .

$$E[n'] = np \quad (\text{B.1})$$

We use an input sequence dependent loss function,  $L^{mr}$ , of each task as shown in Table B.1. We adopt *CrossEntropy* loss function for the Algorithmic, Representation Recall, and bAbI tasks since their input sequences are the binary vectors or one-hot encoding vectors, whereas  $L2$  loss function is adopted to  $N^{th}$  farthest task and the convex hull task because their input data are continuous

values.

Table B.1: The input data dependent loss function,  $L^{mr}$ , for each task.

Task	Algorithmic	Representation Recall	bAbI	$N^{th}$ Farthest	Convex hull
Loss	<i>CrossEntropy</i>			<i>L2</i>	

## Appendix C. Additional Results on bAbI task

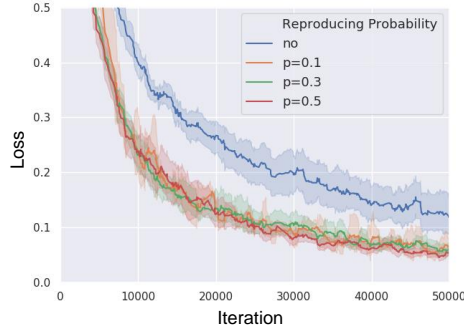


Figure C.1: Mean convergence curves of DAM2-MR for different reproducing probability on the bAbI task. The shadowed area shows a standard deviation of 10 trials.

## Appendix D. Visualization of Distributed Memory Operation (Attentive Gate)

Fig. D.1 and Fig. D.2 show relative weights of multiple memory blocks (DAM-2 and 4) obtained from attentive gate while performing Representation Recall (RR) task. During RR task, the model has to predict missing sub-parts when given other parts as a clue. The figures show how much each sub memory block is referenced when the model is predicting sub-parts. As shown in the above figures, for given tasks, the model effectively integrates well-distributed

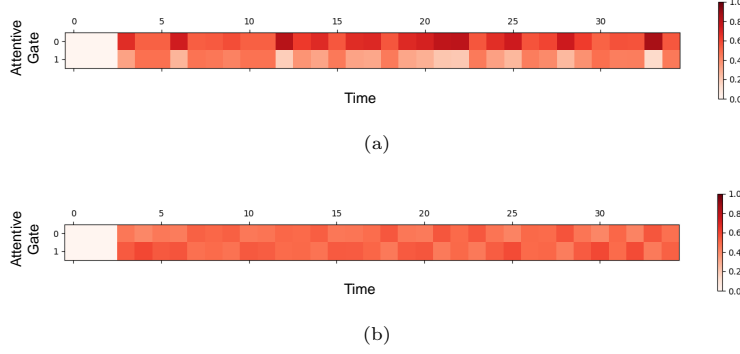


Figure D.1: The activated attentive gate of DAM-2 according to time step on Representation Recall task. (a) 8 sub-parts. (b) 16 sub-parts.

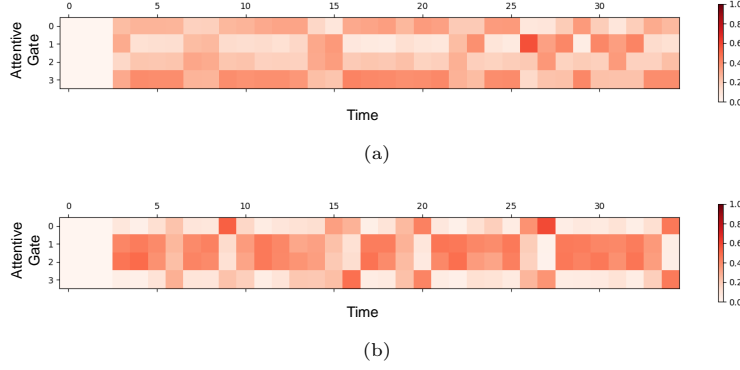


Figure D.2: The activated attentive gate of DAM-4 according to time step on Representation Recall task. (a) 8 sub-parts. (b) 16 sub-parts.

information from multiple memory blocks and utilizing all memory blocks for information retrieval.

## Appendix E. Additional Experimental Analysis on DAM-MR

In the experimental section of our paper, we set up each block size as  $\{A = 64, L = 36\}$  for the copy task and  $\{A = 32, L = 36\}$  for the associative recall task. To show the model performance with a smaller number of memory slots and memory block length, we show the additional experimental analysis.

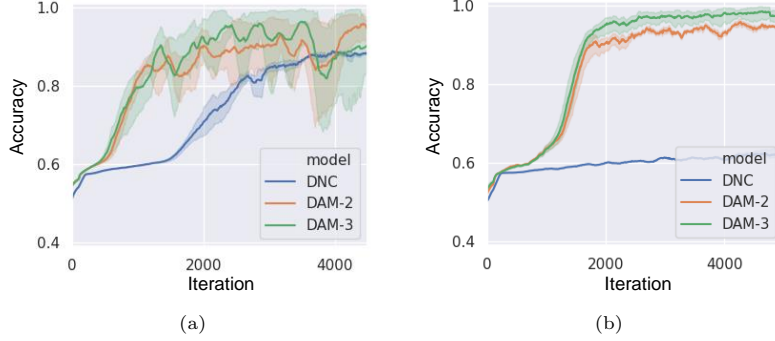


Figure E.1: Mean training curves on the algorithmic tasks with  $A = 16$ , which are (a) the copy task and (b) the associative recall task. The shadowed area shows a standard deviation of 5 trials.

#### Appendix E.1. Experiments with Smaller Memory block Address Size

In our previous Algorithmic experiments, for the copy task, the number of input binary vectors are randomly chosen from  $L_i \in [8, 32]$ , and the memory address size is set up as  $A = 64$ . For the associative recall task, the number of items is chosen from  $L_i \in [2, 8]$  and each input item has  $N_i = 3$  length, and  $A$  is set to 32. In this experiment, we decrease  $A$  from 64 to 16 for the copy task, and from 32 to 16 for the association recall task, so that each memory block has less number of memory slots than the length of the input sequence. Figure E.1 shows DAM performance on the copy and the association recall task according to the number of sub memory blocks. In the results, similar to the previous experiments, the memory network performance on both tasks is enhanced as we increase the number of sub memory blocks.

Figure E.2 shows the experimental result for the effect of MRL on both copy task and associative recall task. In Figs. E.2(a) and (b), even with the decreased number of memory slots,  $A = 16$ , MRL still enhances the DNC and DAM performance on the copy task with increasing reproducing probability. For the associative recall task, the result shows a similar pattern as the copy task.

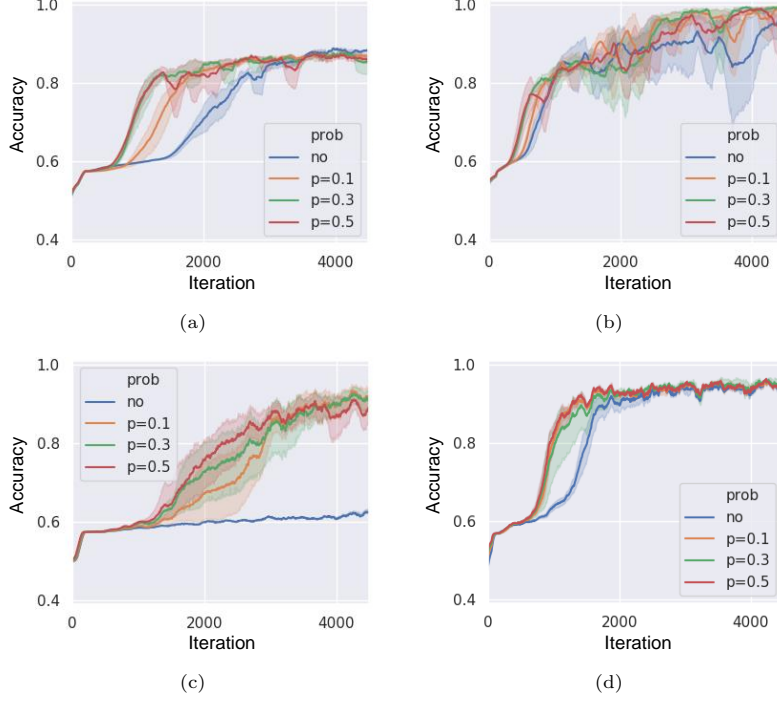


Figure E.2: Mean training curves for different reproducing probability values at (a) DNC and (b) DAM-2 on the copy task with  $A = 16$ . Mean training curves for different reproducing probability values at (c) DNC and (d) DAM-2 on the associative recall task with  $A = 16$ . The shadowed area shows a standard deviation of 5 trials.

## Appendix F. DAM model Equations directly related to DNC

$$(DNC) \ \boldsymbol{\xi}_t = W_{\boldsymbol{\xi}} \mathbf{h}_t = [W_{\boldsymbol{\xi},1}] \mathbf{h}_t \in \mathbb{R}^{L \cdot R + 3L + 5R + 3} \quad (F.1)$$

$$\begin{aligned} (DAM) \ \boldsymbol{\xi}_t = W_{\boldsymbol{\xi}} \mathbf{h}_t &= [\boldsymbol{\xi}_{t,1}, \dots, \boldsymbol{\xi}_{t,K}, \hat{g}_t^{at}] \\ &= [W_{\boldsymbol{\xi},1}, \dots, W_{\boldsymbol{\xi},K}, W_{\boldsymbol{\xi},at}] \mathbf{h}_t \in \mathbb{R}^{K \cdot (L \cdot R + 3L + 3R + 3)} \end{aligned} \quad (F.2)$$

DNC generates the memory operators,  $\boldsymbol{\xi}_t$ , called as interface vector, for its single memory operation, and DAM extends this vector for multiple independent memory blocks. DAM generates  $K$  number of DNC like memory operators,  $\boldsymbol{\xi}_{t,k}$ , (except for temporal linkage operator) and newly introduce attentive gate,  $\hat{g}_t^{at}$  to read from those multiple memory blocks.

$$(DNC) \mathbf{M}_t = \mathbf{M}_{t-1} \circ (\mathbf{E} - \mathbf{w}_t^w \mathbf{e}_t^\top) + \mathbf{w}_t^w \mathbf{v}_t^\top \quad (\text{F.3})$$

$$(DAM) \mathbf{M}_{t,k} = \mathbf{M}_{t-1,k} \circ (\mathbf{E} - \mathbf{w}_{t,k}^w \mathbf{e}_{t,k}^\top) + \mathbf{w}_{t,k}^w \mathbf{v}_{t,k}^\top \quad (\text{F.4})$$

The writing process of DAM is the same as DNC as shown in the above equations, except the same write operation is executed in multiple memory blocks independently at the same time.

$$(DNC) \mathbf{r}_t = \mathbf{M}_t \mathbf{w}_t^r \quad (\text{F.5})$$

$$(DAM) \mathbf{r}_t = \sum_{k=1}^K g_{t,k}^{at} \mathbf{M}_{t,k}^\top \mathbf{w}_{t,k}^r \quad (\text{F.6})$$

where  $g_{t,k}^{at} = \text{Softmax}(\hat{g}_{t,k}^{at})$  for  $k = 1, \dots, K$ .

In the reading process of DAM, the basic reading procedure for each memory block is the same as DNC, but, DAM integrates every read-out value from  $K$  memory blocks into a single distributed representation with an attentive gate. The attentive gate,  $\hat{g}_{t,k}^{at}$ , is a newly introduced part of DAM for the attentive interpolation.

## Appendix G. Model Implementation Details

In this section, we provide more detail of the DAM architecture including well-known neural network generalization techniques that are used in [36].

At each time step  $t$ , the controller, LSTM [1], receives a input,  $\mathbf{x}_t \in \mathbb{R}^{d_i}$ , previous hidden state,  $\mathbf{h}_{t-1} \in \mathbb{R}^{d_h}$ , and previous memory read-out values,  $\mathbf{r}_{t-1} = \{\mathbf{r}_{t-1}^i \in \mathbb{R}^L; 1 \leq i \leq R\}$ , where  $L$  is a memory length size and  $R$  is the number of read heads. Based on these values, the controller updates its internal state,  $\mathbf{h}_t = \text{Controller}([\mathbf{x}_t; \mathbf{r}_{t-1}; \mathbf{h}_{t-1}])$ . Then, layer normalization [43] is applied to the updated internal state. From the normalized internal state  $\mathbf{h}_{t, LN}$ , the controller generates a memory operators,  $\boldsymbol{\xi}_t \in \mathbb{R}^{K*(L*R+3L+3R+3)}$ , which is called interface vector, as follows:

$$\boldsymbol{\xi}_t = [\boldsymbol{\xi}_{t,1}, \dots, \boldsymbol{\xi}_{t,K}, \hat{g}_t^{at}] = [W_{\xi,1}, \dots, W_{\xi,K}, W_{\xi,at}] \mathbf{h}_{t, LN} \quad (\text{G.1})$$

where  $\xi_{t,k} \in \mathbb{R}^{L \times R + 3L + 2R + 3}$  is a memory operator for each memory block,  $K$  is the number of memory blocks,  $k \in \{1, \dots, K\}$ , and  $\hat{g}_t^{at} \in \mathbb{R}^{K \times R}$  is an attentive gate.

The interface vector,  $\xi_{t,k}$ , is split into sub-components, and each sub-component and  $\hat{g}_t^{at}$  are used for each memory's read/write operations as follows:

$$\xi_{t,k} = [\mathbf{k}_{t,k}^w; \beta_{t,k}^w; \hat{\mathbf{e}}_{t,k}; \mathbf{v}_{t,k}; \hat{f}_{t,k}^1, \dots, \hat{f}_{t,k}^R; \hat{g}_{t,k}^a; \hat{g}_{t,k}^w; \mathbf{k}_{t,k}^{r,1}, \dots, \mathbf{k}_{t,k}^{r,R}; \hat{\beta}_{t,k}^{r,1}, \dots, \hat{\beta}_{t,k}^{r,R}] \quad (\text{G.2})$$

- the write-in *key*  $\mathbf{k}_{t,k}^w \in \mathbb{R}^L$ ;
  - the write strength  $\beta_{t,k}^w = \zeta(\hat{\beta}_{t,k}^w) \in [1, \infty)$ ;
  - the erase *values*  $\mathbf{e}_{t,k} = \sigma(\hat{\mathbf{e}}_{t,k}) \in [0, 1]^L$ ;
  - the write-in *values*  $\mathbf{v}_{t,k} \in \mathbb{R}^L$ ;
  - $R$  free gates  $\{f_{t,k}^i = \sigma(\hat{f}_{t,k}^i) \in [0, 1]; 1 \leq i \leq R\}$ ;
  - the allocation gate  $g_{t,k}^a = \sigma(\hat{g}_{t,k}^a) \in [0, 1]$ ;
  - the write gate  $g_{t,k}^w = \sigma(\hat{g}_{t,k}^w) \in [0, 1]$ ;
  - the read-out *keys*  $\{\mathbf{k}_{t,k}^{r,i} \in \mathbb{R}^L; 1 \leq i \leq R\}$ ;
  - the read strengths  $\{\beta_{t,k}^{r,i} = \zeta(\hat{\beta}_{t,k}^{r,i}) \in [1, \infty); 1 \leq i \leq R\}$ ; and
  - the attentive gate  $\{g_{t,k}^{at,i} = \text{Softmax}(\hat{g}_{t,k}^{at,i}) \text{ for } k = 1, \dots, K; 1 \leq i \leq R\}$ .
- where  $\zeta(\cdot)$  denotes a Oneplus function,  $\sigma(\cdot)$  denotes a Sigmoid function and  $\text{Softmax}(\cdot)$  denotes a Softmax function.

Based on those memory operators, the model performs a writing process for each memory block simultaneously. The controller finds a writing address,  $\mathbf{w}_{t,k}^w \in [0, 1]^A$ , where  $A$  is a memory address size, in two ways: (i) a content-based addressing and (ii) a memory usage statistic.

The content-based addressing computes data address as following:

$$\mathcal{C}(\mathbf{M}, \mathbf{k}, \beta)[i] = \frac{\exp\{\mathcal{D}(\mathbf{k}, \mathbf{M}[i, \cdot])\beta\}}{\sum_j \exp\{\mathcal{D}(\mathbf{k}, \mathbf{M}[j, \cdot])\beta\}} \quad (\text{G.3})$$

where  $\mathcal{D}(\cdot, \cdot)$  is the cosine similarity,  $\mathbf{M} \in \mathbb{R}^{A \times L}$  is the memory matrix, and the

$\beta$  controls a strength of the address's sharpness.

Therefore, It finds write-content addresses,  $\mathbf{c}_{t,b}^w \in [0, 1]^A$ , based on the cosine similarity between write-in *keys* and memory values, as follows:

$$\mathbf{c}_{t,k}^w = \mathcal{C}(\mathbf{M}_{t,k}, \mathbf{k}_{t,k}^w, \beta \mathbf{g}_{t,k}^w) \quad (\text{G.4})$$

Next, it finds an allocation address,  $\mathbf{a}_{t,k} \in [0, 1]^A$ , considering current memory usage, such as unused or already read memory space. It determines the retention of the most recently read address's values for each memory block through a memory retention vector,  $\boldsymbol{\psi}_{t,k} \in [0, 1]^A$  and it calculates current memory usage vector,  $\mathbf{u}_{t,k} \in [0, 1]^A$  as follows:

$$\boldsymbol{\psi}_{t,k} = \prod_{i=1}^R (1 - f_{t,k}^i \mathbf{w}_{t-1,k}^{r,i}) \quad (\text{G.5})$$

$$\mathbf{u}_{t,k} = (\mathbf{u}_{t-1,k} + \mathbf{w}_{t-1,k}^w - \mathbf{u}_{t-1,k} \circ \mathbf{w}_{t-1,k}^w) \circ \boldsymbol{\psi}_{t,k} \quad (\text{G.6})$$

where  $\circ$  denotes a element-wise multiplication.

Afterwards,  $\mathbf{a}_{t,k}$  is determined based on current memory usage information as follows:

$$\mathbf{a}_{t,k}[\phi_{t,k}[j]] = (1 - \mathbf{u}_{t,k}[\phi_{t,k}[j]]) \prod_{i=1}^{j-1} \mathbf{u}_{t,k}[\phi_{t,k}[i]] \quad (\text{G.7})$$

where  $\phi_{t,k}$  is a free list which informs indices sorted with respect to memory usage values, i.e.  $\phi_{t,k}[1]$  is the index of the least used address.

The writing address for each memory block,  $\mathbf{w}_{t,k}^w$ , is determined by interpolation between  $\mathbf{c}_{t,k}^w$  and  $\mathbf{a}_{t,k}$ , and each memory block is updated, as follows:

$$\mathbf{w}_{t,k}^w = g_{t,k}^w [g_{t,k}^a \mathbf{a}_{t,k} + (1 - g_{t,k}^a) \mathbf{c}_{t,k}^w] \quad (\text{G.8})$$

$$\mathbf{M}_{t,k} = \mathbf{M}_{t-1,k} \circ (\mathbf{E} - \mathbf{w}_{t,k}^w \mathbf{e}_{t,k}^\top) + \mathbf{w}_{t,k}^w \mathbf{v}_{t,k}^\top \quad (\text{G.9})$$

where  $g_{t,k}^a$  controls a proportion between  $\mathbf{a}_{t,k}$  and  $\mathbf{c}_{t,k}^w$ ,  $g_{t,k}^w$  controls an intensity of writing,  $\circ$  denotes element-wise multiplication and  $\mathbf{E}$  is  $\mathbf{1}^{A \times L}$ .



After all memory blocks are updated, the model executes a reading process for each memory block. It finds out a read address for each memory block,  $\mathbf{w}_{t,k}^{r,i} \in [0, 1]^A$ , as follows:

$$\mathbf{w}_{t,k}^{r,i} = \mathcal{C}(\mathbf{M}_{t,k}, \mathbf{k}_{t,k}^{r,i}, \beta_{t,k}^{r,i}) \quad (\text{G.10})$$

where  $i \in \{1, \dots, R\}$ .

Then, it reads preliminary read-out value,  $\mathbf{r}_{t,k}^i \in \mathbb{R}^L$ , from each memory block and interpolates the preliminary read-out values by  $g_t^{at}$  to produce read-out value,  $\mathbf{r}_t^i \in \mathbb{R}^L$ , as follows:

$$\mathbf{r}_{t,k}^i = \mathbf{M}_{t,k}^\top \mathbf{w}_{t,k}^{r,i} \quad (\text{G.11})$$

$$\mathbf{r}_t^i = \sum_{k=1}^K g_{t,k}^{at,i} \mathbf{r}_{t,k}^i \quad (\text{G.12})$$

where  $g_{t,k}^{at,i}$  controls which memory block should be used for final read-out value.

The read-out values,  $\mathbf{r}^t = \{\mathbf{r}_t^i; 1 \leq i \leq R\}$ , are provided to the controller. As in [36], the model applies drop-out [44] to  $\mathbf{h}_{t,LN}$  with a drop-out probability,  $p_{dp}$ , which is computed as  $\mathbf{h}_{t,dp} = \text{DropOut}(\mathbf{h}_{t,LN} | p_{dp})$ . Finally, the controller produces an output,  $\mathbf{y}_t \in \mathbb{R}^{d_o}$ , along with  $\mathbf{h}_{t,dp}$  and  $\mathbf{r}^t$ , as follows:

$$\mathbf{y}_t = W_y[\mathbf{h}_{t,dp}; \mathbf{r}^t] \quad (\text{G.13})$$